*Int. J. Electrochem. Sci.*, 14 **(2019)** 9459 – 9467, doi: 10.20964/2019.10.14

**International Journal of ELECTROCHEMICAL SCIENCE**
www.electrochemsci.org

*Short Communication*

# Preparation of RGO/NiO Anode for Lithium-ion Batteries

*Shiyi Tian[1,*], Guoxu Zheng[2,*], Qian Liu[2], Mingyuan Ren[2], Jinghua Yin[1]*

[1] School of Science, Harbin University of Science and Technology, Harbin 150080, P. R. China
[2] School of software and microelectronics, Harbin University of Science and Technology, Harbin 150080, P. R. China
[*]E-mail: tsywrqwer@163.com, shandian2008.ok@163.com

*Received:* 10 June 2019 / *Accepted:* 22 July 2019 / *Published:* 30 August 2019

As an efficient and stable energy storage device, lithium-ion batteries (LIBs) have become an important part of today's society and are widely used in production and life. The research on the performance of LIBs is also widely concerned by researchers. The electrode material that plays a decisive role in the performance of the battery is our key research object, and many kinds of new negative electrode materials have been explored. Metal organic frameworks (MOFs) are a type of coordination polymers that have attracted wide attention in recent years [1-2]. With MOFs as the precursor, porous metal oxides and porous carbon materials with a controllable structure can be obtained. As electrode materials, they can significantly improve the electrochemical performance of batteries. Therefore, MOFs have become the preferred material of our new electrode materials. In this paper, hydrothermal method is adopted to prepare spherical porous Ni-MOFs material, which is calcined into metal oxide NiO material, and then its electrical conductivity and electrochemical performance are improved on the basis of retaining spherical pore structure. At the constant current density of 1C, the reversible capacity of NiO material maintains stably at 160mAh/g and the coulomb efficiency reaches 97.12% at 200 circles. In this paper, Ni-MOFs is synthesized with graphene oxide (GO) to generalize GO/Ni-MOFs material, and then it is transformed into reduced graphene oxide (RGO) to obtain RGO/NiO. RGO acts as a soft protective layer of active substances, which greatly improves the structural stability of the electrode during charging and discharging process. At the constant current density of 1C and at 200 circles, the reversible capacity reaches 440mAh/g, the coulomb efficiency reaches 99.49%, and its multiplying power and impedance performance are also very out.

**Keywords:** MOFs, RGO, NiO, LIBs, electrode materials

## 1. INTRODUCTION

In modern society, with the exhaustion of non-renewable energy reserves and the destruction of ecological environment, the development of green new energy has been paid more and more attention by the people. As one of the important equipment for energy storage, LIBs are widely used in our production and life [3-5]. The electrochemical properties of LIBs mainly depend on electrode materials,

and nano-structured materials with high theoretical capacity are proposed as their electrode materials, so as to make them present outstanding electrochemical properties [6-9]. As a new type of electrochemical functional materials, MOFs have attracted people's attention due to their excellent structural properties [10-12]. MOFs are a type of crystalline materials with inorganic and organic structures. Due to its large pore volume and large surface area, it has been widely used in the field of energy storage, gas separation, sensors and catalysis [13-17]. The excellent pore structure and huge specific surface area of Ni-MOFs material studied in this paper make it play a great role in Li-ion negative electrode materials. The large specific surface area enables the electrode material to better contact with the electrolyte, and the excellent channel structure can accelerate the travel speed of lithium ions and promote the rapid diffusion of electrolyte. It can be said that these advantages are tailor-made for lithium-ion battery electrodes [18-20]. Carbon material has good electrical conductivity and flexibility, so it is one of the most commonly used composite matrices. The compound of electrode material and carbon material can greatly improve lithium electrical properties. GO is coated on the surface of MOF by electrostatic adsorption, and the interconnected carbon layers form a conductive network, which improves the charge transfer efficiency of electrodes. The existence of carbon layer and pores can also alleviate the volume expansion of electrode materials. Therefore, the unique structure of Ni-MOFs coated by GO guarantees excellent electrochemical performance as LIBs electrode materials [21-23]. In this paper, Ni-MOFs is compounded with GO to obtain RGO/NiO composites with better structure and high conductivity. At last, the electrochemical properties of NiO and RGO/NiO materials are investigated.

## 2. EXPERIMENTAL

### *2.1 Preparation of Ni-MOFs and NiO*

The preparation steps of Ni-MOFs and NiO are as follows: step 1: weigh 1.279g of nickel hexahydrate nitrate and 0.504g of trimesic acid, dissolve them in 70ml of anhydrous ethanol solution and stir for one hour; step 2: pour the well-stirred polymeric precursor solution into the reaction kettle and put it into the oven, then set the temperature at 160℃ and the reaction time at 24h; step 3: after the reaction is complete, the reactor is taken out, and it is naturally cooled to room temperature Then it is washed with methanol and dried, and finally Ni-MOFs is obtained. Later, Ni-MOFs materials are put into muffle furnace and calcined at 400℃ for 2h to obtain NiO materials.

### *2.2 Preparation of GO/Ni-MOFs and RGO/NiO*

The preparation steps of GO/Ni-MOFs and RGO/NiO are as follows: step 1: GO is dispersed in ethanol solution to obtain solution A; step 2: 1.279g of nickel hexahydrate nitrate and 0.504g of trimesic acid are weighed and fully dissolved in 70ml of methanol solution to obtain solution B; step 3: mix solution A and B, pour them into the reactor, and then put them into the oven. Set the temperature at 160℃ and the reaction time at 24h; Step 4: take out the reactor, naturally cool it to room temperature, wash it with methanol, and dry it to obtain GO/Ni-MOFs. The prepared GO/ Ni-MOFs materials are put into the muffle furnace and calcined at 400℃ for 2h to obtain the RGO/NiO materials.

*2.3 Materials characterization*

The material characterization is tested by X - ray diffraction (XRD) and scanning electron microscope (SEM).

*2.4 Electrochemical measurements*

Electrode sheets are prepared, and the prepared electrode materials, super-p carbon black (conduction additive) and adhesive (PVDF) are uniformly stirred into suspension with N-methyl pyrrolidone (solvent) in a ratio of 8:1:1. The button battery (CR2032) is then assembled in a glove box filled with argon gas by distributing its suspension evenly over circular copper sheets. Finally, the electrochemical properties are tested.

## 3. RESULTS AND DISCUSSION

It can be seen from Fig 1b that Ni-MOFs have a regular spherical characterization structure with a diameter of about 4.4μm, flat and smooth surface structure and even channels. As shown in Fig 1a, Ni-MOFs are uniformly dispersed. SEM scanning results of NiO are shown in Fig 1c and 1d. NiO has a regular spherical structure with a diameter of about 4.0μm, relatively flat surface and uniform pore structure. SEM scanning image of RGO/NiO material is shown in Fig 1e, and it can be seen that the spherical surface of NiO is uniformly coated with a folded GO layer. As shown in its high magnification SEM image (Fig. 1f), the GO layer, like gossamer, uniformly covers the surface of NiO, and the microscopic pore structure on the surface can also be clearly distinguished. Fig 2a shows the XRD patterns of Ni-MOFs，NiO and RGO/NiO. Three very strong diffraction peaks of NiO (PDF 70-1849) correspond to (111), (200) and (220) of metal NiO, respectively, indicating that NiO materials are successfully synthesized. The peak value at 23° indicates the presence of RGO. Therefore, it can be known that RGO/NiO materials are successfully synthesized.

To study the electrochemical behavior of electrode materials during charging and discharging process, new cells with NiO and RGO/NiO as electrodes are tested.

Fig 2b shows the CV curve of a new cell with a NiO electrode. At the beginning, it is a negative scan, and the first largest reduction peak appears in the first circle when the electric potential is 0.4V, which corresponds to the first discharge process of NiO, mainly including the alloying reaction that NiO is reduced to $Ni^0$ and metal Ni further reacts with Li to form Li-Ni alloy, and the discharge peak of 0.45V corresponds to the formation of SEI film [24-25]. According to forward scanning, the first large oxidation peak appears when the electric potential is 1.6V, corresponding to the dealloying process of Li-Ni alloy and the process that metal Ni is oxidized into $Ni^{2+}$ to form NiO [26-27]. Based on the above analysis, the reduction peak echoes the oxidation peak up and down in a cycle, and it can be seen that the redox reaction inside LIBs is a reversible reaction. Fig 2c shows the CV curve of a new cell with an RGO/NiO electrode. At the beginning, it is a negative scan, and the first largest reduction peak appears in the first circle when the electric potential is 1.0V, which corresponds to the process that NiO in RGO/NiO is reduced into Ni [28-29]. The small peak near 0V corresponds to the reaction that $Li^+$ inserts into the carbon layer (RGO) [30]. According to forward scanning, the first large oxidation peak appears

when the electric potential is 2.2V. The oxidation peak and reduction peak of RGO/NiO are very obvious, and the CV curves of the second and third cycles can coincide well, revealing its stable electrochemical performance. After comparing these two materials, it can be found that the CV performance of RGO/NiO material is much higher than that of NiO material.

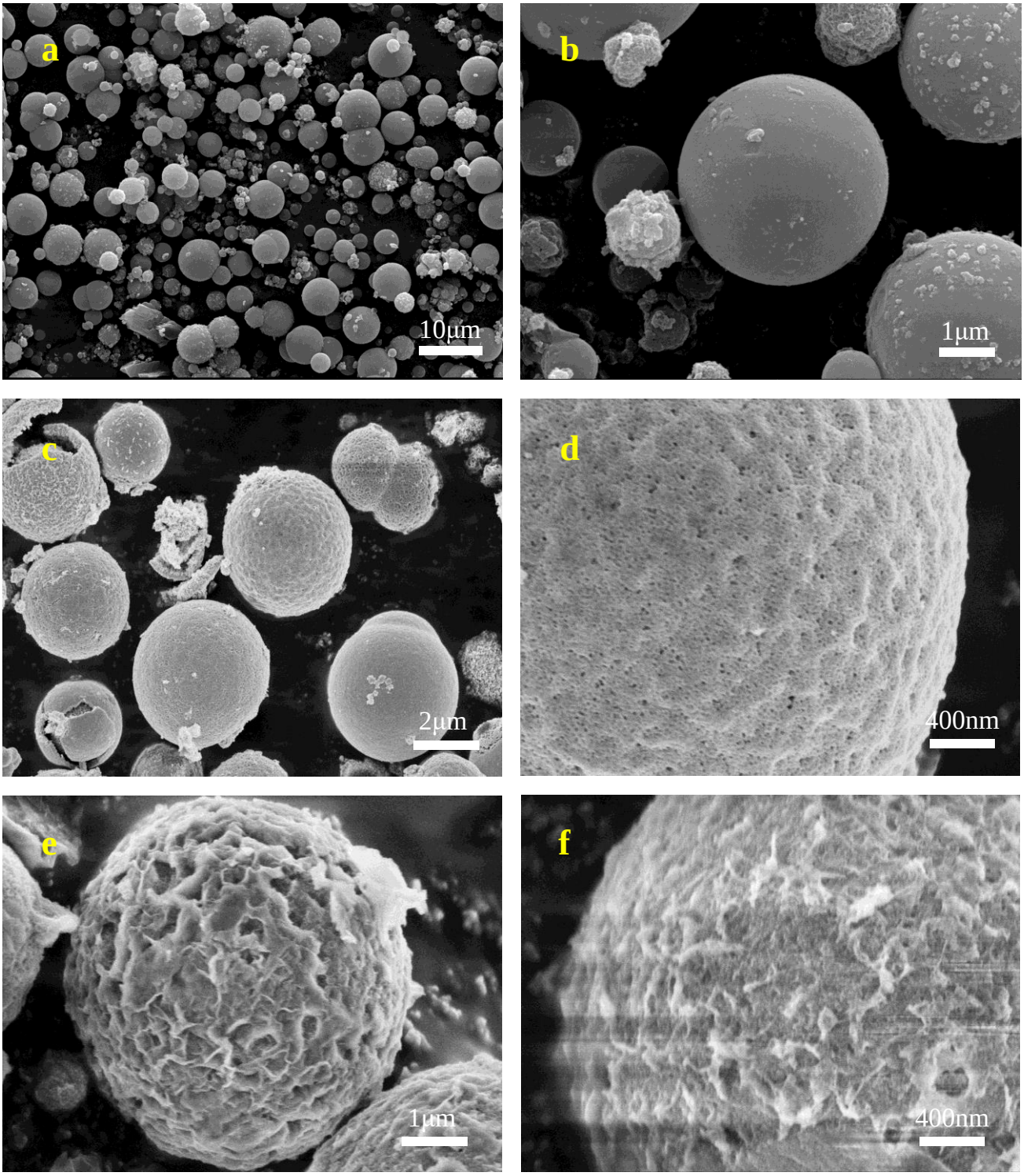


**Figure 1** SEM images of (a-b) Ni-MOFs; (c-d) NiO; (e-f) RGO/NiO

Fig 2d shows the charging and discharging curves of NiO and RGO/NiO. At the current density of 1C, the charge-discharge potential range is set to 0-3V. As can be seen from the Fig, when the electric potential of NiO is about 0.6V, it can be observed that the curvilinear trend is flattening and there is an obvious discharging phenomenon. At this time, lithium ions should be embedded in the electrode, corresponding to the reduction peak in the CV curve. When the electric potential is 1.1V, it can be seen that the curvilinear trend is flattening again, corresponding to the oxidation peak, indicating that it is in the charging process. When the electric potential of RGO/NiO material is about 0.45V, obvious curve changes can be observed. The curvilinear trend is flattening, and there is an obvious discharging phenomenon. At this time, lithium ions should be embedded in the electrode, corresponding to the reduction peak in the CV characteristics. When the electric potential is 1.8V, it can be seen that the curvilinear trend a flattening again, corresponding to the oxidation peak, and at this time, it is in the charging process.

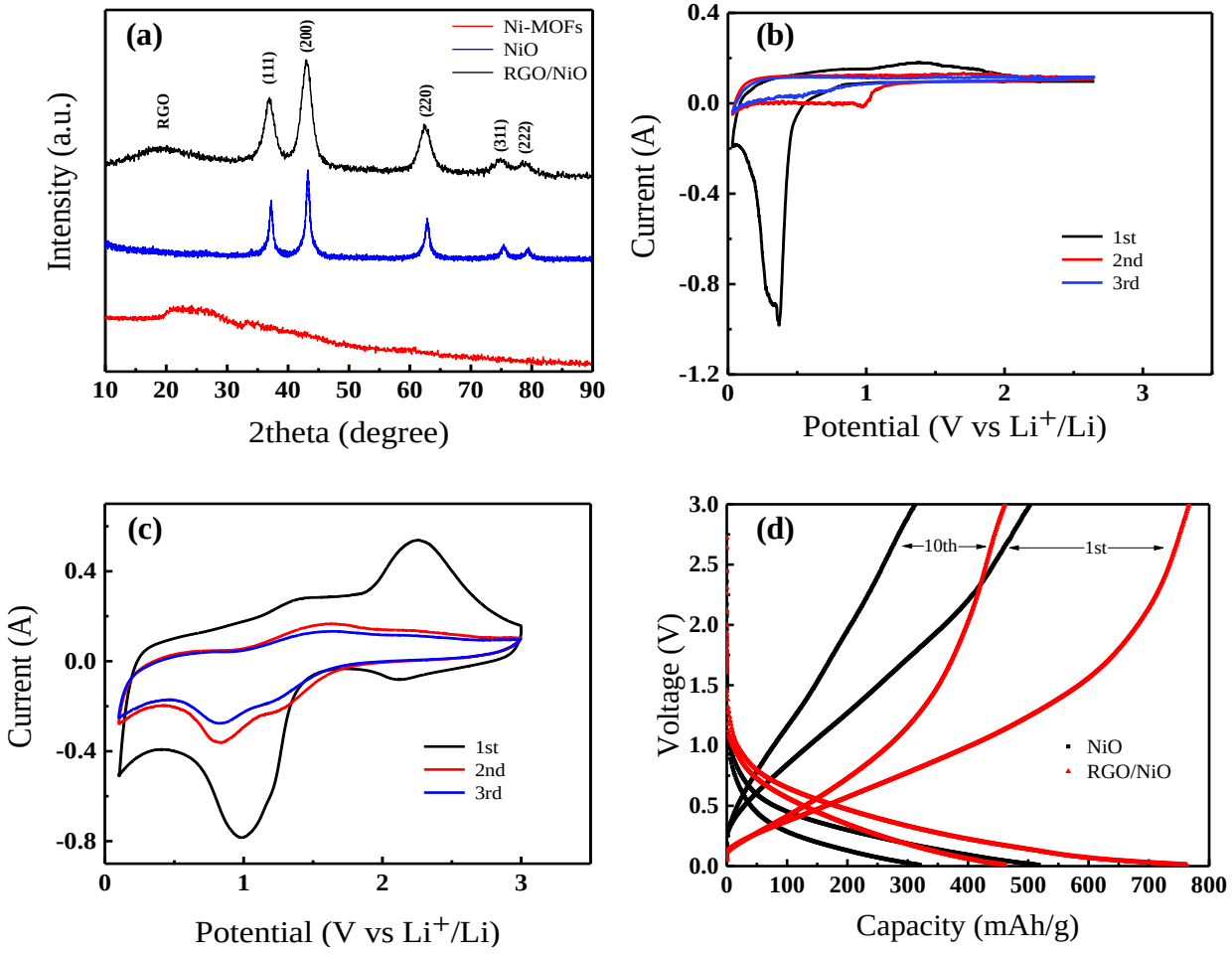


**Figure 2.** (a) XRD patterns of Ni-MOFs, NiO and RGO/NiO; (b) cyclic voltammetry curve of NiO; (c) cyclic voltammetry curve of RGO/NiO; (d) charging and discharging curves of NiO and RGO/NiO

In the first charging and discharging process, the specific discharge capacity of NiO material reaches 517.5372mAh/g, the specific charge capacity reaches 503.1259mAh/g, and the coulombic

efficiency of NiO material reaches 97.12%. While in the first charging and discharging process, the specific discharge capacity of RGO/NiO material reaches 681.5149mAh/g, the specific charge capacity reaches 678.0882mAh/g, and its coulombic efficiency reaches 99.49%. After several cycles, the specific discharge capacity of RGO/NiO material in the tenth time reaches 462.0946mAh/g and the specific charge capacity reaches 461.3245mAh/g. At this time, the specific discharge capacity of NiO material is 320.0073mAh/g, and the specific charge capacity is 312.5024mAh/g. After comparing these two materials, it can be concluded that RGO/NiO material has a much higher specific charge-discharge capacity and coulombic efficiency than NiO material, so its performance is better.

Fig 3a shows the cyclic performance curves of NiO and RGO/NiO. At this time, it is set as 200 times. The initial specific capacity of LIBs with NiO as the electrode material is about 490mAh/g. With the increase of the number of cycles, the capacity of the battery shows a significant decline trend. This is because to the surface area of the electrode at the beginning of the cycle and the battery has irreversible capacity, which corresponds to the formation of SEI film. The battery stabilizes after about 100 cycles, with a capacity of about 160mAh/g. In contrast, RGO/NiO material is used. As shown in the Fig, the initial capacity of lithium ion battery with RGO/NiO material as electrode material is about 670mAh/g, and it stabilizes at 440mAh/g as the number of cycles increases. Although the battery capacity shows a decline trend, the performance is more stable. By comparison, the initial capacity and stable circulation capacity of RGO/NiO material are much higher than those of NiO material, with a smaller downward trend and better performance. Table 1 is a comparison of NiO, RGO/NiO and previously published similar work, further demonstrating that RGO/NiO has good cycle performance.

**Table 1.** Comparison of cycle performance of RGO / NiO materials with other NiO materials with different morphologies

| Typical examples | Current density | Capacity | Ref. |
|---|---|---|---|
| NiO | 100mA/g | 160mAh/g after 200 cycles | This work |
| RGO/NiO | 100mA/g | 440mAh/g after 200 cycles | This work |
| NiO microparticles | 50mA/g | 400mAh/g after 20 cycles | [31] |
| NiO nanosheets | 50mA/g | 210mAh/g after 50 cycles | [32] |
| Flower-like microparticles NiO | 100mA/g | 350mAh/g after 40 cycles | [33] |
| Porous microspheres NiO | 200mA/g | 380mAh/g after 30 cycles | [34] |

Fig 3b and 3c are rate performance curves of NiO and RGO/NiO. During the test, the parameters are set as follows according to the gradient: the test point location is 0-3v, and the scanning rate is 0.1mV/s. In terms of electric current density, the gradient is set as follows: 1c, 2.5c, 4c, 5c, 7.5c, 10c, 1c, and the cycle index is set as 20 times. According to the results, with the increase of the electric current density, the reversible capacity of NiO material under several gradients is 162.356mAh/g, 140.441mAh/g, 117.615mAh/g, 108.556mAh/g, 85.833mAh/g, 62.429mAh/g and 161.713mAh/g, which are significantly lower than the reversible capacity of RGO/NiO material (424.669mAh/g,

341.102mAh/g, 284.705mAh/g, 259.737mAh/g, 204.583mAh/g, 133.851mAh/g and 442.212mAh/g). This is because RGO which not only acts as a conductive layer but also acts as a flexible protective layer fixes the active substances and makes them communicate with each other, so as to avoid falling off in the charging and discharging process.

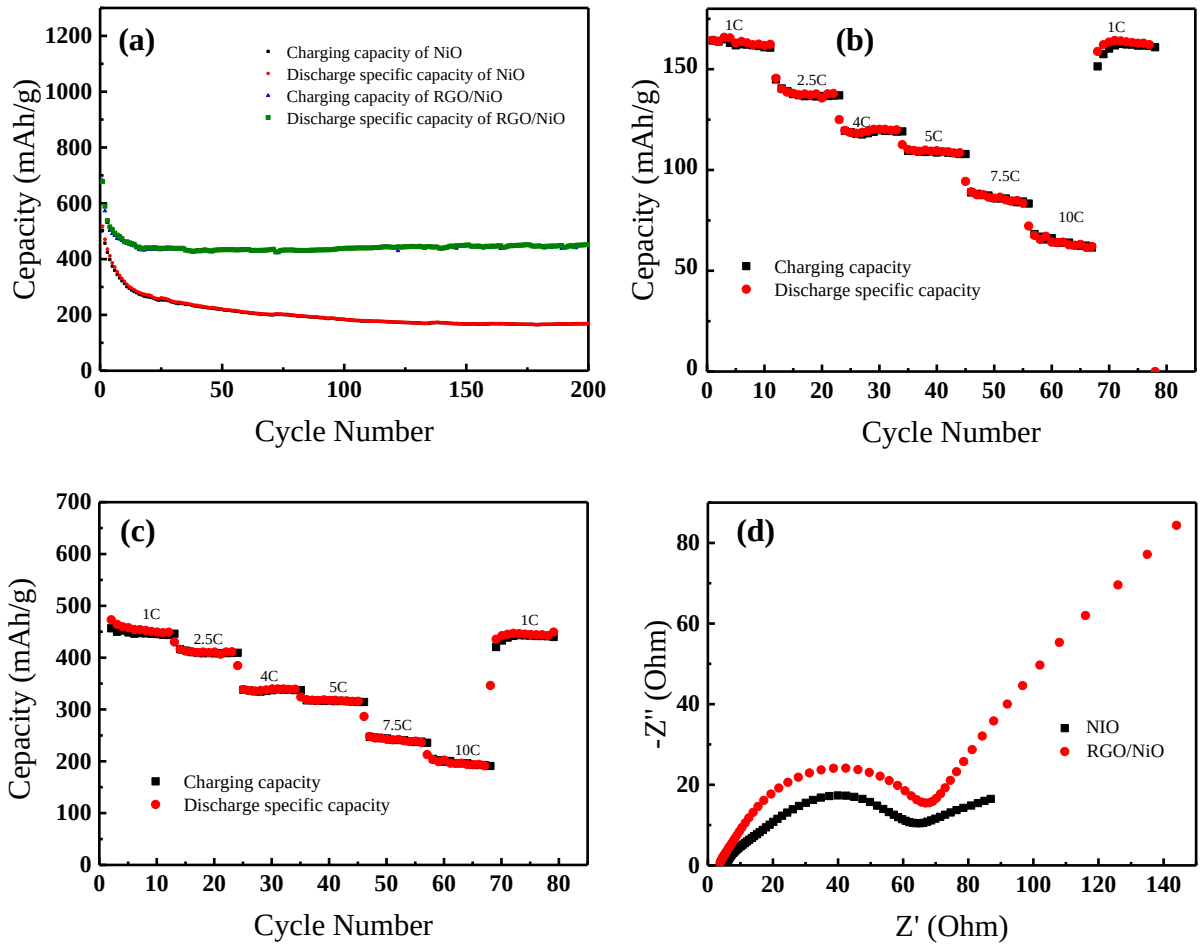


**Figure 3.** (a) cyclic performance curves of NiO and RGO/NiO;(b) rate performance curve of NiO; (c) rate performance curve of RGO/NiO; (d) AC impedance sectroscopy of NiO and RGO/NiO

Fig 3d shows the AC impedance sectroscopy of NiO and RGO/NiO, which is composed of two parts. The semicircle in the high-frequency region is related to the charge transfer process, while the straight line in the low-frequency region reflects the lithium ion transfer process. The diameter of the semicircle in the high-frequency region of RGO/NiO is smaller than the curve radius of NiO, revealing its lower impedance value and higher charge transfer efficiency. This result further verifies the function of graphene layer. RGO covers the surface of NiO and conducts the active substances to each other, which is conducive to the charge transfer in the charging-discharging reactions and enables it to show a high specific capacity at high current rate.

## 4. CONCLUSIONS

The Ni-MOFs material prepared in this paper shows a perfect spherical pore structure and moderate size. The performance of RGO/NiO composite as LIBs electrode is obviously better than that of NiO. At the constant current density of 1C, the capacity stabilizes at 440mAh/g and the coulomb efficiency is up to 99.49% after 200 cycles. RGO/NiO increases the surface lithium storage and specific surface area, and the excellent pore structure guarantees efficient charge transfer efficiency. Moreover, the RGO covering the outer layer acts as a soft protective layer of active substances, which makes the structure not easy to be damaged in the charging and discharging process, so it is better than NiO in terms of circulation, rate and CV performance. In general, RGO/NiO composites are the preferred lithium ion battery cathode materials.

ACKNOWLEDGMENTS
The authors acknowledge financial support from Natural Science Foundation of China (51502063), China Postdoctoral Science Foundation (2016T90306 and 2015M570301), Natural Science Foundation (E2015064) and Postdoctoral Science Foundation (LBH-TZ0615) of Heilongjiang Province of China, Natural Science Foundation of Heilongjiang Province of China (Geant No.F2017017),and Science Funds for Young Innovative Talents of HUST (201505).

## References

1. X.L. Xu, W.H. Shi, P. Li, S.F. Ye, C.Z. Ye, H.J. Ye, T.M. Lu, A.A. Zheng, J.X. Zhu, L.X. Xu, M.Q. Zhong and X.H. Cao, *Chem. Mater.*, 29 (2017) 6058.
2. X.H. Cao, C.L. Tan, M. Sindoro and H. Zhang, *Chem. Soc. Rev.*, 46 (2017) 2660.
3. Y. Cao, F.L. Yuan, M.S. Yao, J.H. Bang and J.H. Lee, *Crystengcomm*, 16 (2014) 826.
4. K.Y. Zou, Y.C. Liu, Y.F. Jiang, C.Y. Yu, M.L. Yue and Z.X. Li, *Inorg. Chem.*, 56 (2017) 6184.
5. Y.G. Wang, Y.F. Song and Y.Y. Xia, *Chem. Soc. Rev.*, 45 (2016) 5925.
6. P. Liu, E. Sherman and A. Jacobsen, *J. Power Sources*, 189 (2009) 646.
7. X.X. Lu, H.C. Fu, F. Han, Y.R. Fang, J.L. Xu, L.Q. Zhang and Q. Du, *J. Thorac. Dis.*, 10 (2018) 1449.
8. M.H. Chen, D.L. Chao, J.L. Liu, J.X. Yan, B.W. Zhang, Y.Z. Huang, J.Y. Lin and Z.X. Shen, *Adv. Funct. Mater.*, 27 (2017) 1606232.
9. M.H. Chen, J.L. Liu, D.L. Chao, J. Wang, J.H. Yin, J.Y. Lin, H.J. Fan and Z.X. Shen, *Nano Energy*, 9 (2014) 364.
10. D. Farrusseng, S. Aguado and C. Pinel, *Angew. Chem. Int. Edit.*, 48 (2009) 7502.
11. H. Furukawa, K.E. Cordova, M. O'Keeffe and OM. Yaghi, *Science*, 341 (2013) 974.
12. T.Q.N. Tran, G. Das and H.H. Yoon, *Sensor. Actuat. B-Chem.*, 243 (2017) 78.
13. D.H. Ge, H.B. Geng, J.Q. Wang, J.W. Zheng, Y. Pan, X.Q. Cao and H.W. Gu, *Nanoscale*, 6 (2014) 9689.
14. R.H. Wang, C.H. Xu, J. Sun and L. Gao, *Sci. Rep-UK.*, 4 (2014) 7171.
15. J.W. Wang, H. Zhang, X.X. Lv, K.Q. Nie, X.J. Gao, J. Zhong and X.H. Sun, *J. Mater. Sci.*, 51 (2016) 6590.
16. J. Lee, O.K. Farha, J. Roberts, K.A. Scheidt, S.T. Nguyen and J.T. Hupp, *Chem. Soc. Rev.*, 38 (2009) 1450.
17. A. Dhakshinamoorthy, M. Alvaro and H. Garcia, *Catal. Sci. Technol.*, 1 (2011) 856.
18. O. Coulembier, T. Josse, B. Guillerm, P. Gerbaux and P. Dubois, *Chem. Commun.*, 48 (2012) 11695.
19. P.B. Gai, H.J. Zhang, Y.S. Zhang, W. Liu, G.B. Zhu, X.H. Zhang and J.H. Chen, *J. Mater. Chem.*

*B.*, 1 (2013) 2742.
20. B. Wang, J.L. Cheng, Y.P. Wu, D. Wang and D.N. He, *Electrochem. Commun.*, 23 (2012) 5.
21. X. Wang, Q.X. Wang, Q.H. Wang, F. Gao, F. Gao, Y.Z. Yang and H.X. Guo, *Acs Appl. Mater. Inter.*, 6 (2014) 11573.
22. R.K. Srivastava, S. Srivastava, T.N. Narayanan, B.D. Mahlotra, R. Vajtai, P.M. Ajayan and A. Srivastava, *Acs Nano*, 6 (2012) 168.
23. B.H. Qu, L.L. Hu, Q.H. Li, Y.G. Wang, L.B. Chen and T.H. Wang, *Acs Appl. Mater. Inter.*, 6 (2014) 731.
24. X.F. Li, D.S. Geng, Y. Zhang, X.B. Meng, R.Y. Li and X.L. Sun, *Electrochem. Commun.*, 13 (2011) 822.
25. Q.S. Xie, F. Li, H.Z. Guo, L.S. Wang, Y.Z. Chen, G.H. Yue and D.L. Peng, *Acs Appl. Mater. Inter.*, 5 (2013) 5508.
26. M. Ahmad, Y.Y. Shi, A. Nisar, H.Y. Sun, W.C. Shen, M. Wei and J. Zhu, *J. Mater. Chem.*, 21 (2011) 7723.
27. M.S. Wu and H.W. Chang, *J. Phys. Chem. C*, 117 (2013) 2590.
28. W. Luo, X.L. Hu, Y.M. Sun and Y.H. Huang, *J. Mater. Chem.*, 22 (2012) 8916.
29. J. Bai, X.G. Li, G.Z. Liu, Y.T. Qian and S.L. Xiong, *Adv. Funct. Mater.*, 24 (2014) 3012.
30. X.F. Li, D.S. Geng, Y. Zhang, X.B. Meng, R.Y. Li and X.L. Sun, *Electrochem. Commun.*, 13 (2011) 822.
31. Y. Cai, J.M. Ma and T.H. Wang, *J. Alloy. Compd.*, 582 (2014) 328.
32. G.M. Zhou, D.W. Wang, L.C. Yin, N. Li, F. Li and H.M. Cheng, *Acs Nano*, 6 (2012) 3214.
33. Q. Li, Y.J. Chen, T. Yang, D.N. Lei, G.H. Zhang, L. Mei, L.B. Chen, Q.H. Li and T.H. Wang, *Electrochim. Acta*, 90 (2013) 80.
34. D. Xie, W.W. Yuan, Z.M. Dong, Q.M. Su, J. Zhang and G.H. Du, *Electrochim. Acta*, 92 (2013) 87.